Numerical investigation of the spreading-receding cycle in a concentration-dependent lattice gas automaton diffusion model

Michel Küntz*
[1]*CRIB, Department of Civil Engineering, Laval University, Québec City, Quebec, Canada G1K 7P4*

Paul Lavallée
Physics Department, UQAM, C.P. 8888, Succursale Centre Ville, Montreal, Quebec, Canada H3C 3P8
(Received 14 July 2004; revised manuscript received 19 January 2005; published 15 June 2005)

This work forms the second part of a numerical study about the dynamics of diffusive fronts in concentration-dependent diffusion processes. We previously demonstrated that one-dimensional spreading of a density front in a concentration-dependent microscopically heterogeneous, macroscopically homogeneous isotropic lattice gas automaton (LGA) substantially deviates from the $t^{1/2}$ relation expected from Fick's law over large periods of time. The time exponent was found to be larger than $1/2$, i.e., spreading of the density front is enhanced with respect to standard Fickian diffusion. In this note, we specifically investigate the dynamics of receding by using the same LGA model. We show here that the receding process essentially scales as $t^{1/2}$. The LGA simulations of diffusive fronts thus lead to the paradoxical result of Fick's-compatible receding and anomalous superdiffusive spreading for the same microscopic random structure and the same boundary conditions. The results also suggest that hysteresis of the spreading-receding cycle could arise from the contrasted dynamics between spreading and receding. A conceptual model of "offer and demand" which includes both the diffusivity gradient $dD(\rho)/d\rho$ and the conditions applied at boundaries as main parameters is proposed to tentatively account for the dynamics of diffusive fronts in concentration-dependent diffusion processes.

DOI: 10.1103/PhysRevE.71.066703 PACS number(s): 02.70.Ns, 02.60.Lj, 05.60.Cd, 81.05.Rm

I. INTRODUCTION

Diffusion is present everywhere, from ionic transport in biological membranes to moisture transfer in nonsaturated porous media [1,2]. While numerous theoretical and experimental studies have been already devoted to depict this transport mechanism in the past, the dynamics of diffusive front remains a challenging and continuously renewed problem with very important practical applications in all fields of sciences. Classically, the analysis of diffusion has been conducted at the macroscopic level by using the empirical Fick's hypothesis, which stipulates proportionality between the flux q and the concentration gradient: $q=D\nabla C$, where D is the coefficient of diffusion and C the concentration of the diffusing quantity. The main implication of Fick's assumption has been pointed out early: the displacement rate of the diffusing quantity (or the velocity of the diffusing front) must be proportional to the square root of time in one dimension, provided that the system considered is homogeneous and isotropic [3,4]. It is worth noting that the $t^{1/2}$ scaling imposed by Fick's hypothesis remains equally valid whether the coefficient of diffusion is constant or varies with the concentration of the diffusing quantity and whether diffusive fronts are spreading or receding fronts [3]. The $t^{1/2}$ dependence of diffusive fronts is in fact considered as the fingerprint of diffusion and has been systematically used to detect the occurrence of this transport mechanism in natural processes. It is inversely assumed that any diffusionlike process which does not follow the expected $t^{1/2}$ relation cannot be diffusion alone. In the past two decades however, evidence of deviation from the classical $t^{1/2}$ relation has been increasingly often reported in almost all fields of sciences (see [5] and references herein). It has been possible in some circumstances to relate deviation from the $t^{1/2}$ scaling to the spatial and/or temporal variations of the transport properties of the physical system considered [6]. In most cases, however, the spatial and/or temporal variation of the diffusion coefficient was not established and the anomaly essentially remained unexplained. The ever-growing evidence of nonclassical behavior (generally referred to as "anomalous diffusion") attracted a large attention and progressively led to question the overall validity of Fick's theory of diffusion [7–9].

We recently proposed that anomalous diffusion may systematically occur in concentration-dependent diffusion processes, i.e., processes in which the diffusion coefficient $D(C)$ is a function of the concentration C of the diffusing quantity [5,10]. We used a concentration-dependent lattice gas automaton (LGA) diffusion model to simulate diffusion in a microscopically heterogeneous random structure and we demonstrated that spreading of a density front substantially and systematically deviates from the expected $t^{1/2}$ scaling over both short and large periods of time in this model. It should be mentioned that the same result was previously obtained by [11] from Monte Carlo simulations of a similar problem. We were also capable to relate occurrence of anomalous spreading to the diffusivity gradient $dD(C)/dC$ in the concentration-dependent LGA diffusion model: positive and negative diffusivity gradients are expected to lead to superdiffusive and subdiffusive spreading respectively. It is worth noting that the results of numerical simulations have been since corroborated by experimental data. Spreading of

*Electronic address: michelkuntz@gmail.com

moisture fronts in nonsaturated porous media provides several examples of superdiffusion [13–16,20], whereas evidence of subdiffusion has been reported in concentrated $CuSO_4$ solution diffusing in pure water [5,17]. Both simulations and experiments thus suggest that anomalous spreading of diffusive fronts is the rule in concentration diffusion processes.

In this note, we used the LGA model introduced in [10] to specifically investigate the process of receding of a density front in order to get a complete picture of the spreading-receding cycle in concentration-dependent diffusion processes. One of the objectives was to determine whether the dynamics of receding was also anomalous or whether it is compatible with the $t^{1/2}$ time scaling inferred from Fickian hypothesis. The simulations carried out indicate that receding essentially scales as $t^{1/2}$ in the one-dimensional semi-infinite LGA model, i.e., the time dependence inferred from Fick's hypothesis remains valid for the receding case at first glance. We also show that the complete spreading-receding cycle as simulated through the concentration-dependent LGA diffusion model naturally presents hysteresis. The note is organized as follows: the basic features of the LGA model and numerical techniques used to simulate concentration-dependent diffusive fronts are briefly sketched in Sec. II. The numerical evidence that supports the $t^{1/2}$ dependence of the receding process is reviewed in Sec. III. The numerical results are discussed in Sec. IV. We compare the evolution in time of the receding and spreading processes to definitively establish that (i) the two processes do not follow the same dynamics and (ii) the variations of the dynamics of diffusive fronts from spreading to receding can only be related to the difference of the conditions applied at the boundaries in the LGA model. Numerical evidence of hysteresis of the spreading-receding cycle is also provided in this section. The contrasted behavior between spreading and receding diffusive fronts is tentatively reconciled by applying the "offer and demand" model introduced in [10]. We show that anomalous spreading and normal receding is expected if the diffusivity gradient $dD(C)/dC$ is positive. In this scheme, the receding process should be subdiffusive in concentration-dependent diffusion processes where the diffusivity is a continuously decreasing function of the concentration.

II. THE NUMERICAL MODEL

Over the past decade, the lattice gas automaton (LGA) method has proven to be a reliable numerical tool to simulate hydrodynamics and diffusion processes [18,19]. The LGA method and its theoretical principles have been extensively described in previous publications to which the reader is referred and will not be reminded here except for the very basic lines. Schematically, the macroscopic behavior of a lattice gas automaton is the result of the collective behavior of many individual discrete particles which locally follow the same simple and invariable interaction rules. All the particles have unit mass and travel at unit velocity on a discrete triangular lattice and they may engage in collisions which allow redistribution of their velocities along the directions of the lattice but must conserve the mass and momentum of the particles: the continuity and momentum conservation are thus locally satisfied at any time. It is now well established that the LGA are capable to simulate Navier-Stokes and diffusion equations at the macroscopic level [19]. The macroscopic transport properties of the gas are determined by the collision rate which control how mass and momentum are redistributed in the triangular lattice. The probability of collisions depends of course on the applied collision rules but also on the concentration of the particles in the lattice, i.e., the intrinsic diffusivity of the LGA is a direct function of the concentration ρ. This makes LGA a suitable tool to investigate concentration-dependent diffusion processes, as already pointed out in [12]. The concentration ρ used below is defined as the average number of particles per lattice site: $\rho=0$ corresponds to an empty lattice (no particles), whereas $\rho=1$ indicates that every site of the triangular lattice houses a particle. Because all the particles have the same velocity, the temperature is constant and the equation of state simplifies to a linear relationship between the pressure P and the density of particles ρ, i.e., there is a direct correspondence between pressure and concentration.

The simulations were conducted using the same model as that described in [10]: only the initial state of the lattice and the conditions applied at the boundaries have been changed. The two-dimensional triangular lattice was 8000 lattice units (l.u.) long and $200\sqrt{3}/2$ l.u. large. The microscopically heterogeneous, macroscopically homogeneous isotropic medium was identically approximated by point scatterers distributed at random which populate 8% of the lattice sites. Particles were interacting following the FHP_5 collision rules [21] [in reference to the Frisch, Hasslacher, and Pomeau (FHP) lattice gas automaton model, Frisch *et al.*, Phys. Rev. Lett. **56**,1505 (1986)] and free slip specular reflection was applied at the interface between the scatterers and the particles [22]. As previously noted in [12], the effective diffusivity $D(\rho)$ of the microscopically heterogeneous LGA model is a function of both the applied interparticles collisions rules and the interaction of the particles with the scatterers. The variation of $D(\rho)$ was estimated in [10] for the specific combination of collisions used in this paper and is represented in Fig. 1 as a function of ρ. The diffusion coefficient $D(\rho)$ is a decreasing function of ρ at very low concentration, remains almost constant between $\rho=0.05$ and $\rho=0.5$ and then increases by about two decades from $\rho=0.5$ to $\rho=0.85$.

The particles were initially distributed at a uniform concentration $\rho_1=0.9$ with an average velocity $\langle u\rangle=0$ over all the triangular lattice, i.e., each site was close to its maximum capacity at $t=0$ (Fig. 2). The boundaries are periodic in the y direction: the particles that leave at one side re-enter the lattice on the other side with the same direction and velocity. To simulate one-dimensional receding in a semi-infinite medium, a concentration drop was imposed by maintaining a constant concentration $\rho_0=0.01$ along the right-hand side of the model ($x=8000$) during the simulation, while the left-hand side ($x=0$) was hermetically closed. In response to the applied density drop $\rho_1-\rho_0$, the particles naturally migrate toward the low concentration boundary where they are allowed to escape freely at the interface. As a result, the lattice

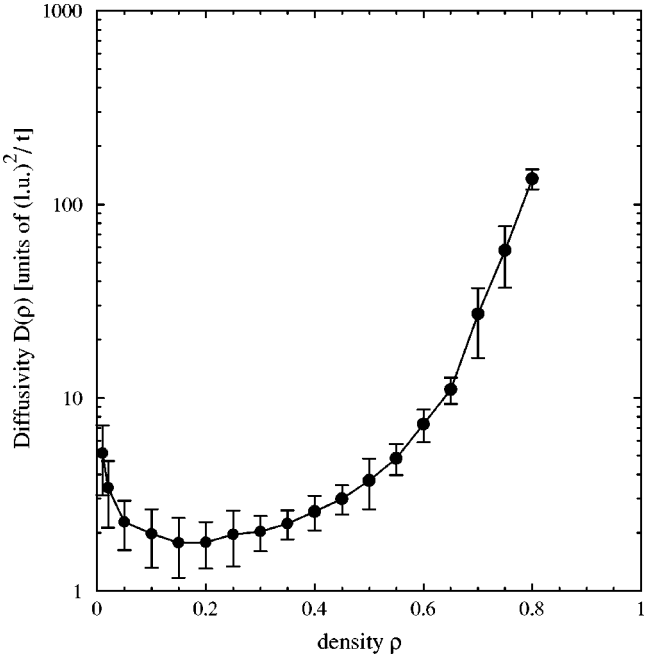

FIG. 1. Effective diffusivity of the LGA model implemented in this paper as a function of the density of particles ρ.

progressively empties: this in turn induces receding of the density front.

III. NUMERICAL RESULTS

Receding of the density front was monitored as a function of time in Fig. 3. The density profiles were obtained by summing all the particles over all y at each position x for a given t and the procedure was repeated at different time steps. As soon as the particles are free to leave the triangular lattice, a steep knee-shaped front forms. Then, the front progressively

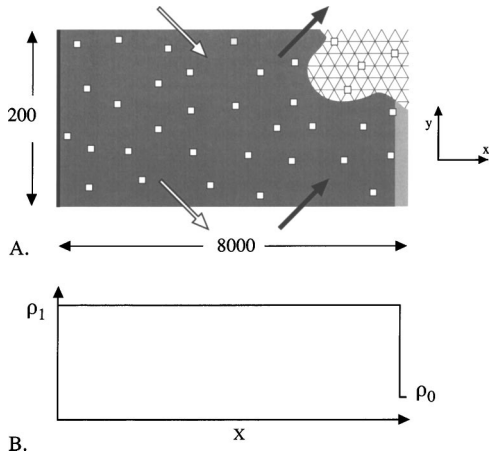

FIG. 2. (a) Schematic view of the numerical setup. White squares figure scatterers randomly distributed in the lattice, clear and dark gray zones represent, respectively, low and high particle's concentration. The arrows illustrate the periodic boundaries along the y direction. (b) Concentration profile at $t=0$ along the x direction.

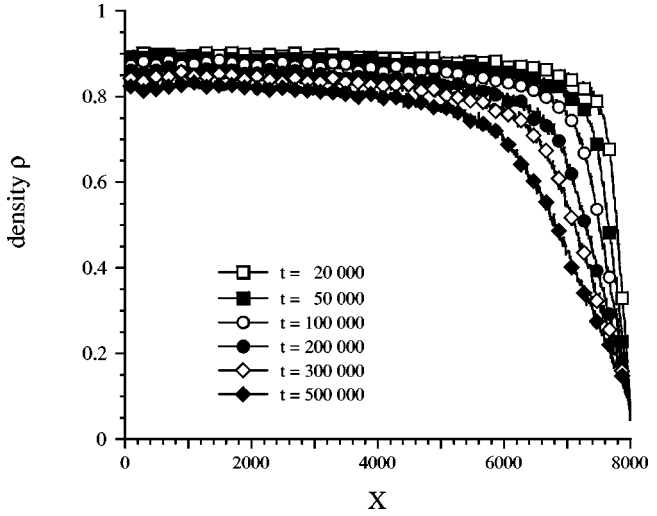

FIG. 3. Position of the receding front at different time steps of the simulation.

moves back inside the heterogeneous medium toward the left-hand side of the model. The slope of the density front progressively smoothes as time elapses but the concentration of particles remains constant along the left-hand side, i.e., the model remains semi-infinite during the first 100 000 time steps. Then, the receding front finally reaches the left side of the universe and the average concentration gradient applied at the boundaries starts to decrease: the receding process is not semi-infinite anymore. The particles continue to leave the lattice until the medium eventually empties, i.e., the concentration gradient becomes null. The simulation was however stopped after 500 000 time steps before draining was completed because of prohibitive calculation times.

The dynamics of receding was determined by evaluating the particles flow rate through the open boundary as a function of time. The number of remaining particles was measured every 10 time steps by summing all the particles in the lattice. This quantity was then subtracted from the initial number of particles to determine the cumulative loss of mass. The result is reported in a log-log diagram in Fig. 4. The "instantaneous" slope of the cumulative mass loss curve was calculated over successive intervals of a few thousands time steps from the curve of Fig. 4 and is reported in Fig. 5. As can be seen, the slope is initially significatively larger than $1/2$, but rapidly decreases to reach $1/2$ after a few thousands time steps. The slope then remains almost constant until the simulation was stopped with only small fluctuations around the value $1/2$. It is important to mention that the slope remains constant after the receding front has reached the left-hand side of the model, i.e., after the concentration drop $\rho_1-\rho_0$ initially imposed at the boundaries has started to decrease, suggesting that the way the receding process evolves in time does not depend on the value of the applied concentration gradient.

Evolution with time of the momentum of the particles provides complementary information by allowing us to evaluate the forces at play during the receding process. The momentum curve of Fig. 6 was calculated by summing the x component of the momentum mv_x of all the particles over all

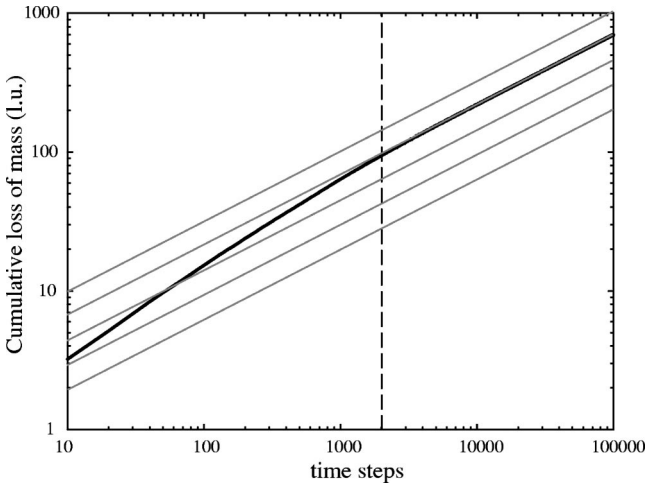

FIG. 4. Illustration of the cumulative particles loss as a function of time (log-log diagram). The slope of the gray lines is $\frac{1}{2}$. The dashed line approximatively indicates the time at which receding starts to scale as $t^{1/2}$.

lattice sites every 10 time steps. The concentration of remaining particles was also plotted in the same diagram. Note that because the model is one-dimensional, the mean value of the y component of the momentum remains close to 0 all the time. The momentum, which is null at $t=0$ (the mean velocity of the particles $\langle v\rangle=0$ at $t=0$) initially increases abruptly once the density drop is established, reaches a maximum after a few thousands time steps and then starts to decrease continuously, as the front progressively smoothes. The mean particles velocity follows the same trend, i.e., it increases first, then stabilizes before showing a slow and regular decrease as time elapses. On the other hand, the force responsible for the displacement of the particles toward the open boundary continuously decreases with time and the resulting forces acting on the receding front become negative after a few thousands time steps. The initial impulsion which

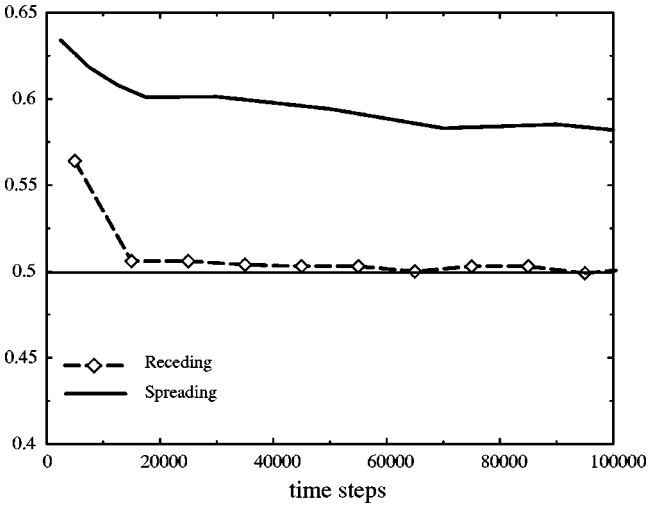

FIG. 5. Evolution with time of the slope a of the cumulative mass loss curve of Fig. 4. The slope of the cumulative mass gain curve as measured during the spreading simulations in [10] is also reported for comparison.

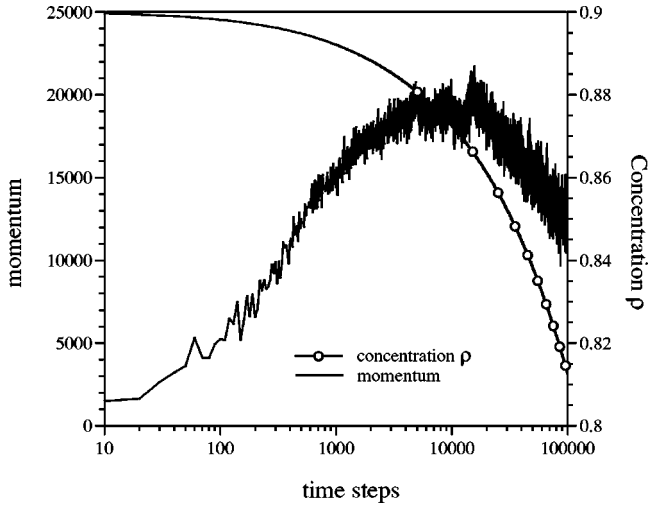

FIG. 6. Evolution of the cumulative momentum of the particles populating the microscopically heterogeneous medium against time.

results from the application of an infinite concentration gradient at $t=0$ thus continuously dissipates. The origin of this force and its evolution with time will be tentatively clarified in the next section.

IV. DISCUSSION

The results reported above indicate that one-dimensional receding of a density front essentially scales as $t^{1/2}$ in the concentration-dependent diffusion lattice gas automaton, except for the first few thousands time steps (Fig. 5). As far as the LGA model is representative of the dynamics of diffusive fronts in concentration-dependent diffusion problems, the $t^{1/2}$ dependence of the receding process inferred from the classical empirical Fick's law (see for instance [2,4]) thus applies. While it may be argued that such a result barely deserves a mention, it must be compared with the previous findings of the authors about spreading in the same LGA model [10]. Indeed, we recently established that the expected $t^{1/2}$ relation did not hold to account for spreading. To illustrate this, we plotted the evolution of the slope of the cumulative infiltration curve (i.e., the gain rate of particles) measured during spreading simulations in [10] as a function of time in Fig. 5 for comparison. It must be reminded that the applied boundary conditions were identical for the two numerical experiments, which only differed by the initial particle's content. It is evident from the diagram that the two processes, receding and spreading, do not follow the same dynamics. Whereas in the former case the time exponent remains close to $1/2$ most of the time, it is significatively larger than $1/2$ in the latter case [10]. This leads to the paradoxical result of "normal," Fick's-compatible receding and anomalous superdiffusive spreading.

One consequence of the contrasted dynamics between receding and spreading processes could be hysteresis of the spreading-receding cycle. To validate this assumption that has intuitively been inferred from the previous results, both the receding and spreading experiments were repeated until the diffusion regime became stationary, i.e., the number of

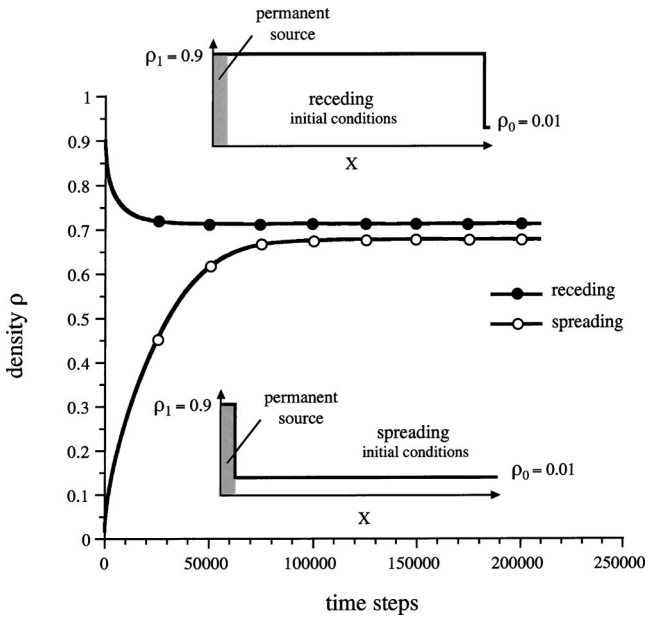

FIG. 7. Evolution of the number of particles as a function of time for both the receding and spreading numerical experiments. The stationary regime is established after about 50 000 and 100 000 time steps, respectively. The number of remaining particles in steady state is clearly different whereas the conditions applied along the boundaries are identical for the two simulations. The initial and boundary conditions of the experiments are illustrated by the two diagrams included in the figure.

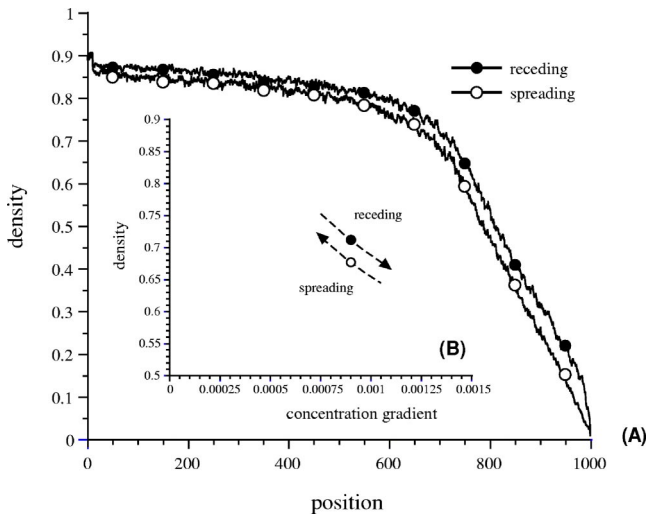

FIG. 8. (a) A comparison of the steady-state concentration profiles for both receding and spreading. (b) A representation of the steady-state concentration as a function of the applied concentration gradient. The data suggest a hysteresis loop with the spreading branch lying below the receding branch as expected from experiments.

particles leaving the lattice on the right-hand side was the same as that entering the model on the left-hand side (see Fig. 2). In order to obtain a steady state, a continuous source of particles at a constant concentration was required along one boundary for both spreading and receding simulations (Fig. 7). Note also that a smaller, 1000×200 lattice was used to reduce calculation times. The conditions applied at the boundaries in both cases were the same as those described in Sec. II otherwise (i.e., $\rho_0 = 0.01$ and $\rho_1 = 0.9$; see Fig. 2). Evolution with time of the density of particles is plotted in Fig. 7 for the two experiments. As can be seen, the density does not change anymore after 50 000 and 100 000 time steps for receding and spreading, respectively, indicating that the LGA diffusion model has reached a stationary regime. However, the density of the particles populating the lattice in steady state is not the same in both cases (Fig. 7): it is actually lower for spreading than for receding by about 4%. The origin of such a difference was clarified by comparing the spreading and receding steady-state density profiles in Fig. 8(a). Although the two profiles present a similar knee-shaped envelope, they actually do not superimpose. The particles density along the spreading profile is systematically lower at any given x position: as a consequence, the spreading front lies below the receding one close to the right open boundary. The mean density of particles in steady state was evaluated for the two numerical experiments by integrating the two profiles over x and plotted in Fig. 8(b) as a function of the concentration gradient applied at the boundaries. As expected, the two points do not coincide: the density point associated with receding lies significatively above that for spreading by about 4%, for the same applied density gradient $\rho_1 - \rho_0$. The diagram suggests the existence of a complete hysteresis loop with the spreading branch lying below the receding branch: this is actually the classical geometry of hysteresis loops measured experimentally. It should be mentioned here that to determine numerically a complete hysteresis loop would have required large calculation times as well as substantial modifications of the code in order to be able to scan a large range of density gradients: a more complete data set will be hopefully presented in a forthcoming paper. It must be reminded that hysteresis was initially not the objective of these simulations: occurrence of hysteresis actually appears as an emerging property of the diffusing process in the concentration-dependent LGA diffusion model.

The problem then arises to know how receding does scale as $t^{1/2}$ and spreading does not. It should be mentioned here that this question has not been fully clarified yet. As specified in the introduction, diffusion equation of the type $\partial C/\partial t = \nabla \cdot [D(C) \nabla C]$ cannot give solutions which do not scale as $t^{1/2}$: the validity of such a statement is corroborated in many reference works (see for instance [3]) and we were able to verify it on our own with both analytical and numerical approaches. The generally well-accepted idea that anomalous diffusion in microscopically heterogeneous media arises from the interactions of the diffusing quantity with the complex fractal geometry of the background (see [9]) should be rejected in this case: (i) as pointed out earlier [10], the geometry of the microscopically heterogeneous LGA is not fractal (the scatterers are randomly distributed) and (ii) the same microscopically heterogeneous random structure was used for both receding and spreading experiment, whereas only spreading was found to be anomalous. It is of particular importance at this stage to remind oneself that the dynamics of the particles at the "microscopic" level were governed by identical rules (FHP_5 collision rules between the particles

and specular "free-slip" collisions against the scatterers) for both the receding and spreading experiments, i.e., the elementary mechanisms of mass and momentum transfer remain unchanged at the particles level. Since the difference in the macroscopic dynamics of the concentration front between spreading and receding does not reflect a change of the modes of interactions between the particles, the variations of the dynamics of diffusive fronts must then be looked for in the conditions applied at the boundaries of the LGA model.

The apparently inconsistent results of "normal," Fick's-compatible receding and anomalous superdiffusive spreading can be tentatively reconciled through the model of "offer and demand," initially introduced by Küntz and Lavallée [10] to account for anomalous spreading in concentration-dependent diffusion processes. Spreading can be viewed as the inflation of the source (which can be continuous in time or not), i.e., the size of the source continuously increases as the front progresses. The term source used above refers globally to the reservoir from which the particles which progress into the medium come from: it corresponds in practice to the domain where the concentration of the particles is higher than the initial concentration or/and higher than the concentration imposed along the open boundary. The way the source inflates results from the competition between its potential of expansion and the capacity of the front to move forward. The result of this competition is settled by the diffusivity gradient, i.e., the spatial distribution of the transport properties inside the inflating source, as previously proposed in [10]. For a positive $dD(\rho)/d\rho$, as for the LGA model described in this note (see Fig. 1 and also Ref. [10]), the expansion of the source is limited at the front because of the small diffusivity at low concentration. Because the number of particles provided behind the front is larger than what can be propagated at the front, the spreading front actually behaves as if it were pushed and superdiffusion occurs. The numerical results reported in the previous section indicate that receding is initially driven by the same mechanism. Because $dD(\rho)/d\rho > 0$, the pressure immediately builds up behind the front once the concentration drop has been established along the open side of the model: and as for spreading, the receding front initially behaves as if it were pushed. Evidence of the pressure buildup inside the source is provided by the initial increase of momentum (Fig. 6). As a consequence, the escape rate of particles is enhanced with respect to that expected from Fick's assumption: offer is larger than demand. This interpretation is corroborated by the fact that the time exponent associated with receding is initially larger than $1/2$ (Fig. 5) as for spreading. However, receding does not involve a mass loss only: the particles that leave the model also carry away momentum with them. The loss of momentum contributes to efficiently dissipate the overpressure induced by the inflation of the source behind the front. The momentum is seen to increase first as inflation occurs and then starts to decrease slowly after only a few thousands time steps, meaning that the overpressure is dissipating (Fig. 6). Note that the momentum peak coincides with the moment at which the time exponent reaches the value $1/2$. After dissipation of the excess pressure, offer can by no way be larger than demand and receding thus scales as $t^{1/2}$.

The same transport mechanism is thus involved for both spreading and receding. The occurrence of "normal" or anomalous diffusion only depends whether momentum resulting from the inflation of the source can be dissipated or not. As a consequence, receding scales as $t^{1/2}$ after only a short period whereas spreading remains superdiffusive over large periods of time. The occurrence of nonclassical "anomalous" spreading in the LGA model therefore essentially reduces to a boundary problem. This in turn implies that the theoretical explanations involving partial differential equation of fractional order (i.e., biased microscopic rules of mass and momentum transfer, see [9]), are not necessary to account for anomalous diffusion in concentration-dependent diffusion processes.

TABLE I. Expected relationships between the type of diffusion, the diffusivity gradient, and the applied boundary conditions, according to the "offer and demand" model. The variable a represents the frontal growth exponent of diffusion.

Diffusivity gradient	Spreading	Receding
$dD(\rho)/d\rho > 0$	superdiffusion	normal diffusion
	$a > \frac{1}{2}$	$a = \frac{1}{2}$
$dD(\rho)/d\rho \approx 0$	normal diffusion	normal diffusion
	$a = \frac{1}{2}$	$a = \frac{1}{2}$
$dD(\rho)/d\rho < 0$	subdiffusion	subdiffusion
	$a < \frac{1}{2}$	$a < \frac{1}{2}$

The predictions that have been inferred from the "offer and demand" analysis are summarized in Table I. If the diffusivity gradient is negative $[dD(\rho)/d\rho < 0]$, diffusion is expected to be subdiffusive for both spreading and receding according to the mechanism of offer and demand, because transport at the front remains always more efficient than behind the front. In this scheme, "true" Fickian diffusion (i.e., diffusion scaling as $t^{1/2}$ all the time) only holds for D constant, i.e., when offer behind the front exactly balances demand at the front. Although the "offer and demand" mechanism essentially remains a "hand waving" conceptual model at this stage, it can account for most of the features of diffusion: it is worth mentioning that its capacity to provide reliable predictions has already been confirmed by experimental data [5,10]. It should be mentioned that it might be that for some physical systems, the diffusivity will not be a simple monotonic increasing or decreasing function of the concentration ρ, but will show several minima and maxima. Prediction of the macroscopic behavior of diffusive fronts in such systems is far from being straightforward at this stage. Both the dynamics and the shape of the front may exhibit mixed features: subdiffusive knee-shaped spreading fronts may be one of these mixed modes for instance [14,23]. Anyway, such problems deserve a more careful and detailed analysis than that presented above.

The "offer and demand" mechanism which only implies a few measurable macroscopic parameters suggests simple experimental tests. The next step of this work will thus consist in confirming the predictions listed in Table I by experiments. Among the many possibilities, investigating the dynamics of moisture fronts in nonsaturated porous media seems the most promising approach. Evidence of anomalous

diffusion of absorption fronts has been already reported in several porous materials [12,14,23]. An experimental investigation is now required to confirm beyond question that receding actually scales as $t^{1/2}$ after only a short period in the materials already investigated. It should be mentioned that drying generally exhibits two distinct stages (e.g., [24]) that may eventually correspond to the two, first anomalous and then normal, regimes identified in LGA receding simulations. Validation of hysteresis is a bit more complex and requires techniques such as nuclear magnetic resonance or radiography to visualize diffusive fronts. According to the LGA simulations, spreading and receding steady-state fronts are expected to be distinct. Since such techniques are now more easily accessible, to reproduce experimentally the simulations reported in previous paragraphs should be in principle straightforward.

V. CONCLUSION

A concentration-dependent LGA diffusion model has been used to investigate the dynamics of diffusive fronts in microscopically heterogeneous macroscopically homogeneous isotropic random structures. We previously established that the $t^{1/2}$ scaling expected from Fick's law did not hold for one-dimensional spreading of a density front in the LGA model. The time exponent was found to be larger than $1/2$, i.e., spreading of the density front was found to be enhanced with respect to standard Fickian diffusion. In this paper, we demonstrated that in contrast with spreading, the receding process scales as $t^{1/2}$ in the same LGA model, after only a short transient period, i.e., spreading and receding do not obey the same dynamics. Since the difference between spreading and receding can only result from the changes of the conditions applied at the boundaries, the occurrence of nonclassical anomalous diffusion therefore reduces to a boundary problem in concentration-dependent diffusion processes. The numerical results also suggest a general mechanism for hysteresis.

ACKNOWLEDGMENTS

Michel Küntz is deeply indebted to his former colleagues, Armel Boutard, Jean Chevalier, Gilles Couture, Cherif Hamzaoui, and Pierre Riopelle from the now defunct department of Physics at UQAM for their help, support, and discussions during the course of this research.

[1] J. Darnell, H. Lodish, and D. Baltimore, *Molecular Cell Biology* (Scientific American Books, Inc., New York, 1986).
[2] J. Philip, Adv. Hydrosci.. **5**, 215 (1969).
[3] J. Crank, *The Mathematics of Diffusion* (Clarendon Press, Oxford, 1975).
[4] H. S. Carslaw and J. C. Jaeger, *Conduction of Heat in Solids* (Clarendon Press, Oxford, 1973).
[5] M. Küntz and P. Lavallée, J. Phys. D **37**, L5 (2004).
[6] B. Berkowitz and H. Sher, Water Resour. Res. **31**, 1461 (1995).
[7] H. Pascal, Physica A **192**, 562 (1993).
[8] D. H. Zanette, Braz. J. Phys. **29**, 108 (1999).
[9] D. Ben Havraham and S. Havlin, *Diffusion and Reactions in Fractal and Disordered Systems* (Cambridge University Press, Cambridge, England, 2000).
[10] M. Küntz and P. Lavallée, J. Phys. D **36**, 1135 (2003).
[11] R. Nassif, Y. Boughaleb, A. Hekkouri, J. F. Gouyet, and M. Kolb, Eur. Phys. J. B **1**, 453 (1998).
[12] M. Küntz and P. Lavallée, J. Phys. D, **34** 2547 (2001).
[13] M. Küntz, P. Lavallée, J. Chevalier, P. Riopelle, and M. Goyer, in *Masonry: Opportunities For the 21st Century*, edited by D. Throop and R. E. Klingner (ASTM, West Conshohocken, PA, 2002), STP 1432, p. 259.
[14] A. El-Ghany El Abd and J. J. Milczarek, J. Phys. D **37**, 2305 (2004).
[15] P. Mansfield, R. Botwell and S. Blackband, J. Magn. Reson. (1969-1992) **99**, 507 (1992).
[16] P. M. Smith and M. M. Fisher, Polymer **25**, 84 (1984).
[17] A. E. Carey, S. W. Wheatcraft, R. J. Glass, and J. P. O'Rourke, Water Resour. Res. **31**, 2213 (1995).
[18] G. R. McNamara, Europhys. Lett. **12**, 329 (1990).
[19] D. Rothman and S. Zaleski, *Lattice Gas Cellular Automata*, Collection Alea-Saclay (Cambridge University Press, Cambridge, England, 1997).
[20] M. Küntz, J. G. M. van Mier, and P. Lavallée, Transp. Porous Media, **43**, 289 (2001).
[21] M. Bonetti, A. Noullez, and J. P. Boon, in *Cellular Automata and Modeling of Complex Physical Systems*, edited by P. Manneville *et al.* (Springer, Berlin, 1989), p. 239.
[22] P. Lavallée, J. P. Boon, and A. Noullez, in *Discrete Kinematic Theory, Lattice Gas Theory and Foundations of Hydrodynamics*, edited by R. Monaco (World Scientific, Singapore, 1989), p. 206.
[23] I. A. Guerrini and D. Swartzendrüber, Soil Sci. Soc. Am. J. **56**, 335 (1992).
[24] L. Pel, K. A. Landman, and E. F. Kaasschieter, Int. J. Heat Mass Transfer **45**, 3173(2002).